J. Fluid Mech. (2001), *vol.* 438, *pp.* 1–10. Printed in the United Kingdom

Convection in a horizontally heated sphere

By G. D. McBAIN

School of Engineering, James Cook University, Townsville, Queensland 4811, Australia

(Received 17 January 2000 and in revised form 22 November 2000)

Natural convection in horizontally heated spherical fluid-filled cavities is considered in the low Grashof number limit. The equations governing the asymptotic expansion are derived for all orders. At each order a Stokes problem must be solved for the momentum correction. The general solution of the Stokes problem in a sphere with arbitrary smooth body force is derived and used to obtain the zeroth-order (creeping) flow and the first-order corrections due to inertia and buoyancy. The solutions illustrate the two mechanisms adduced by Mallinson & de Vahl Davis (1973, 1977) for spanwise flow in horizontally heated cuboids. Further, the analytical derivations and expressions clarify these mechanisms and the conditions under which they do not operate. The inertia and buoyancy effects vanish with the Grashof and Rayleigh numbers, respectively, and both vanish if the flow is purely vertical, as in a very tall and narrow cuboid.

1. Introduction

We consider here natural convection in the fluid filling a small horizontally heated spherical cavity in a conducting solid. Apart from applications such as closed-cell insulation (Lewis 1950), the problem is interesting because it is a fully three-dimensional example of internal natural convection which permits some analytical progress. Here the low Grashof number expansion is calculated to zeroth and first orders, clarifying known three-dimensional flow features of the analogous problem in a cuboid as studied by, for example, Mallinson & de Vahl Davis (1973, 1977).

Buoyancy-driven flow in a horizontally heated spherical cavity has been studied independently by Lewis (1950) and Ostroumov (1958), in connection with gas bubbles in foam insulating materials and the geothermics of underground reservoirs, respectively. As in the present paper, the analysis centred on the asymptotic expansion for low Grashof numbers. Lewis and Ostroumov both argued that the flow would be confined to the parallel family of planes defined by the directions of gravity and heating. As will be demonstrated in § 4, this is only correct in the creeping flow limit. This erroneous assumption makes their work useless for the present purpose: the illumination of three-dimensional features of buoyancy-driven cavity flows. The problem of the sphere seems not to have been returned to since these two early studies.

1.1. *Generation of spanwise flow*

The three-dimensional nature of low Grashof number flow in horizontally heated cavities can be marked. For finite cuboids this was first predicted by the numerical solutions of Mallinson & de Vahl Davis (1973, 1977) and later observed in the experiments of Morrison & Tran (1978) and Hiller, Koch & Kowalewski (1989). In 1973 Mallinson & de Vahl Davis explained the effect purely in terms of the reduction of the convective disturbance of the temperature field by the viscous damping of the endwalls but in 1977 they postulated a second mechanism: the inertial interaction of

a rotating mass of fluid and a stationary solid wall, by analogy with the work of Pao (1970) on the fluid confined in a rotating cylinder with one stationary endwall.

It is primarily to clarify these mechanisms for spanwise flow that the present investigation was undertaken. Some qualifications of published conclusions (Mallinson & de Vahl Davis 1977; de Vahl Davis 1998) on the inertial mechanism in cuboids are required. In particular, it will be seen that the mechanism is not quite universal; it would not occur if the vertical aspect ratio were so large that the presence of the floor and ceiling could be ignored, nor if the Grashof number were so low that terms $O(Gr)$ might be neglected. Since de Vahl Davis's conclusions were based on the examination of numerical solutions with finite values of the vertical aspect ratio ($1 \leqslant A \leqslant 5$) and Grashof number ($Gr$ no less than a few hundred), there is no contradiction or paradox here, merely an elucidation of the correct asymptotic behaviour.

If the entire boundary of a fluid were rotating, the fluid, at steady state, would rotate as a solid body (Rayleigh 1913), in which case the effect of the centrifugal force would be to generate a pressure varying as the square of the azimuthal velocity (Lamb 1932, p. 28). With one endwall fixed, the azimuthal velocity (and therefore the centrifugal force and consequent pressure) must vary axially. It is this axial variation in pressure which gives rise to the axial velocity. Now, the centrifugal force is inversely proportional to the radius of curvature of the azimuthal velocity. In the rotating cylinder this is simply equal to the distance from the axis, but in a buoyancy-driven cavity flow, this need not be so. For a unicellular flow in a very tall cavity (McBain 1999*a*) the streamlines sufficiently far from the horizontal surfaces will be practically straight, so that their radius of curvature is infinite and the centrifugal force vanishes. There is, therefore, no centrifugally generated pressure, no axial variation of centrifugally generated pressure and no force to cause axial flow. The centrifugal force is proportional to the square of the azimuthal velocity, and therefore must vanish faster than the primary circulating flow as the speed scale tends to zero. Thus, the inertial mechanism for spanwise flow in a confined convective roll vanishes if either the streamlines are straight or terms quadratic in the velocity become negligible.

The buoyancy mechanism for flow in the third dimension also depends on the curvature of the primary flow. It is the turning of the basic buoyancy-induced vertical flow by the ceiling and floor that redistributes the temperature and distorts the buoyancy, to a greater degree near the $z = 0$ plane and less so near the 'endwalls'. Thus this mechanism too is inoperative for unicellular flow in a tall slender cavity. The recent analytical solutions for the tall slender cavity (McBain 1999*a*) indeed show a purely vertical flow. It was to reconcile these unidirectional solutions with the observed three-dimensional behaviour in vertically bounded cavities that the present work was originally undertaken. This has been accomplished.

The results of the present study of the sphere fully support the contentions of this section. In § 2 the equations governing the asymptotic expansion for low Grashof numbers are derived from the full Boussinesq equations. An analytical method for solving the resulting momentum equations is detailed in § 3, and used in § 4 to obtain the solutions for the creeping flow and its first-order corrections.

2. Problem formulation

2.1. *Governing equations*

For a sphere of diameter D subjected to a horizontal temperature difference ΔT and gravitational field strength $-g\hat{\boldsymbol{j}}$, and filled with a fluid of density ρ, kinematic viscosity ν, thermal diffusivity α, and thermal coefficient of cubic expansion β, a

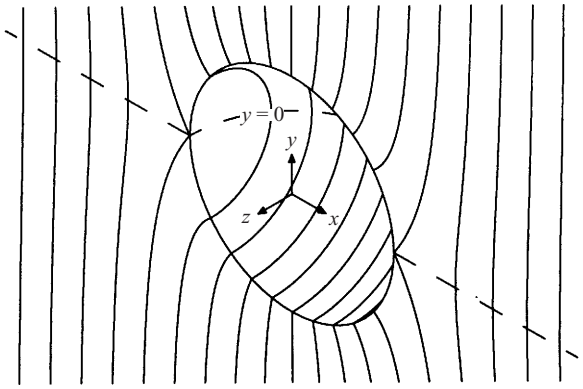

FIGURE 1. The geometry, sliced in the plane of symmetry $z = 0$, showing isotherms in the surrounding solid and on the boundary of the sphere $r = \frac{1}{2}$ for $z < 0$.

suitable Grashof number is $Gr = g\beta\Delta T D^3/\nu^2$. Taking D, $D^2/\nu Gr$, $\rho D^3/Gr$ and ΔT as the scales of length, time, mass and temperature, the Boussinesq equations governing steady heat transfer and flow are

$$Gr\ Pr\ \boldsymbol{u}\cdot\nabla T = \nabla^2 T, \tag{2.1a}$$

$$Gr\ \boldsymbol{u}\cdot\nabla\boldsymbol{u} = -\nabla p + T\hat{\boldsymbol{j}} + \nabla^2\boldsymbol{u}, \tag{2.1b}$$

subject to

$$\nabla\cdot\boldsymbol{u} = 0. \tag{2.1c}$$

Here, $\boldsymbol{u}$ is the velocity and p and T are the excesses of the pressure and temperature, respectively, over their values at the centre of the cavity. The y-direction, with unit vector $\hat{\boldsymbol{j}}$, has been chosen as vertical (see figure 1*a*). The Prandtl number is defined by $Pr = \nu/\alpha$.

2.2. *Geometry and boundary conditions*

It is convenient to work with spherical polar coordinates relative to either the positive z-axis, (r, θ, ϕ), or the positive y-axis, (r, η, υ) with unit vectors $\hat{\boldsymbol{r}}, \hat{\boldsymbol{\phi}}$, etc. The relation of the Cartesian axes to the imposed temperature gradient is illustrated in figure 1.

Ostroumov's (1958) study is more general than the present in that the former includes the finite conductivity of the surrounding solid. Since solids are often better conductors than fluids, let us assume for simplicity that the solid is infinitely conducting. If the temperature gradient in the solid far from the cavity is uniform and horizontal (parallel to the x-axis), the temperature at the boundary of the sphere is analogous to the flow potential on a solid sphere moving along the x-axis through a perfect fluid, i.e. it varies linearly with x (Lamb 1932, p. 123), though the gradient differs from that in the far solid. Explicitly, the temperature field

$$T = \frac{1}{3}\left(\frac{1}{8r^3} + 2\right) r\sin\theta\cos\phi \tag{2.2}$$

is harmonic outside the sphere $r = 1/2$, and equals x and has zero normal gradient on its surface. Far from the sphere, $T \sim \frac{2}{3}x$. The temperature field in the surrounding solid is shown in figure 1.

The linear temperature variation was proposed by Lewis (1950) and Ostrach (1988) on the grounds that it 'corresponds to that which would occur in the solid without gas bubbles' (Ostrach 1988), which (apart from the factor $\frac{2}{3}$) is true but irrelevant.

2.3. *The low Grashof number expansion*

For fixed Pr, expand $\boldsymbol{u}$, p and T as power series in Gr, e.g. $\boldsymbol{u} \sim \boldsymbol{u}_0 + Gr\ \boldsymbol{u}_1 + Gr^2\boldsymbol{u}_2 + \cdots$, and substitute into the full equations (2.1). The limit $Gr \to 0$ gives a hierarchy of problems:

$$Pr \sum_{k=0}^{i-1} \boldsymbol{u}_{i-1-k} \cdot \nabla T_k = \nabla^2 T_i, \tag{2.3a}$$

$$T_i = \begin{cases} x & (i = 0) \\ 0 & (i = 1, 2, \ldots) \end{cases} \qquad (r = \tfrac{1}{2}), \tag{2.3b}$$

and

$$\nabla \cdot \boldsymbol{u}_i = 0, \tag{2.4a}$$

$$\sum_{k=0}^{i-1} \boldsymbol{u}_{i-1-k} \cdot \nabla \boldsymbol{u}_k - T_i \hat{\boldsymbol{j}} = -\nabla p_i + \nabla^2 \boldsymbol{u}_i, \tag{2.4b}$$

$$\boldsymbol{u}_i = \boldsymbol{0} \quad (r = \tfrac{1}{2}). \tag{2.4c}$$

Solution of the heat equations is straightforward. For the equations of motion, however, the presence of the unknown pressure terms and the continuity constraints means that at each order a Stokes problem with known 'body force' must be solved. This is treated in the following section.

3. Solution of the Stokes equations in a sphere

A technique is described here for reducing the Stokes problem in a sphere to an uncoupled unconstrained set of scalar partial differential equations (Poisson and inhomogeneous biharmonic equations). It is based on decomposing the velocity field into poloidal and toroidal parts. The essential properties of the decomposition are summarized here; further details can be found in McBain (1999*b*) and the references therein. In brief, a toroidal field is a solenoidal field with no radial component and a poloidal field is a solenoidal field with a toroidal curl. The main new result of this section is the general solution of the Stokes equations in a sphere for an arbitrary smooth body force.

3.1. *Solenoidal fields*

Chadwick & Trowbridge (1967) proved that any vector field, $\boldsymbol{v}$, sufficiently smooth and solenoidal in a spherical shell, can be there expressed $\boldsymbol{v} = (\nabla\times)^2\,(\mathscr{P}[\boldsymbol{v}]\boldsymbol{r}) + \nabla \times (\mathscr{T}[\boldsymbol{v}]\boldsymbol{r})$, where $\boldsymbol{r}$ is the position vector and $\mathscr{P}[\boldsymbol{v}]$ and $\mathscr{T}[\boldsymbol{v}]$ are scalar fields, obtained as the regular solutions of (Moffatt 1978, p. 18)

$$\mathscr{L}^2 \mathscr{P}[\boldsymbol{v}] \equiv \left(r^2\nabla^2 - \frac{\partial}{\partial r} r^2 \frac{\partial}{\partial r} \right) \mathscr{P}[\boldsymbol{v}] = -\boldsymbol{r} \cdot \boldsymbol{v} \tag{3.1}$$

and

$$\mathscr{L}^2\, \mathscr{T}[\boldsymbol{v}] = -\boldsymbol{r} \cdot \nabla \times \boldsymbol{v}. \tag{3.2}$$

It has been shown by Backus (1986) that the lemma can be extended from spherical annuli to spheres.

3.2. *Non-solenoidal fields*

While the velocity fields of interest here are all solenoidal, the inertia and buoyancy forces can have non-zero divergence. A general vector field (of sufficient smoothness) can be decomposed as follows.

LEMMA 1 (Decomposition of vector fields). *Any vector field, $\boldsymbol{v}$, sufficiently smooth in a sphere, can be there expressed:*

$$\boldsymbol{v} = \nabla\mathscr{S}[\boldsymbol{v}] + (\nabla\times)^2(\mathscr{P}[\boldsymbol{v}-\boldsymbol{v}^{(S)}]\boldsymbol{r}) + \nabla\times(\mathscr{T}[\boldsymbol{v}-\boldsymbol{v}^{(S)}]\boldsymbol{r}). \tag{3.3}$$

Proof. Define the scalar field $\mathscr{S}[\boldsymbol{v}]$ as the solution of the problem

$$\nabla^2\mathscr{S}[\boldsymbol{v}] = \nabla\cdot\boldsymbol{v} \quad (0\leqslant r<\tfrac{1}{2}), \tag{3.4a}$$

$$\boldsymbol{r}\cdot\nabla\mathscr{S}[\boldsymbol{v}] = \boldsymbol{r}\cdot\boldsymbol{v} \quad (r=\tfrac{1}{2}), \tag{3.4b}$$

and let

$$\boldsymbol{v}^{(S)} \equiv \nabla\mathscr{S}[\boldsymbol{v}]. \tag{3.5}$$

Then, $\boldsymbol{v}-\boldsymbol{v}^{(S)}$ is solenoidal and can be decomposed into poloidal and toroidal parts as in § 3.1. □

Following Elsasser (1946) $\boldsymbol{v}^{(S)}$ is called the *scaloidal* part of $\boldsymbol{v}$. Similarly, $\boldsymbol{v}^{(P)} \equiv \nabla\times\nabla\times\left(\mathscr{P}[\boldsymbol{v}-\boldsymbol{v}^{(S)}]\boldsymbol{r}\right)$ and $\boldsymbol{v}^{(T)} \equiv \nabla\times\left(\mathscr{T}[\boldsymbol{v}-\boldsymbol{v}^{(S)}]\boldsymbol{r}\right)$ are called the *poloidal* and *toroidal* parts of $\boldsymbol{v}$.

3.3. *Boundary conditions*

For $\boldsymbol{v}^{(T)} = \boldsymbol{0}$ on a spherical surface, $\mathscr{T}[\boldsymbol{v}]$ must be uniform over the surface. Since any function of r can be subtracted from $\mathscr{T}[\boldsymbol{v}]$ without affecting $\boldsymbol{v}^{(T)}$, this constant can be taken as zero without loss of generality.

For $\boldsymbol{r}\cdot\boldsymbol{v}^{(P)} = 0$ on a spherical surface,

$$\mathscr{L}^2\mathscr{P}[\boldsymbol{v}] = 0 \quad \text{(on the surface)}. \tag{3.6}$$

Since the only regular solutions of this equation are functions only of r (Padmavathi, Raja Sekhar & Amaranth 1998, Lemma 2) and any such function can be subtracted from $\mathscr{P}[\boldsymbol{v}]$ without affecting $\boldsymbol{v}^{(P)}$, we can require $\mathscr{P}[\boldsymbol{v}] = 0$ on the surface.

For a poloidal velocity field to satisfy the no-slip condition, $\partial\mathscr{P}/\partial r$ must be uniform over the surface. Again, there is no loss of generality in requiring it to vanish.

3.4. *The Stokes problem in the sphere*

We are now in a position to derive the general solution of the inhomogeneous Stokes problem in the sphere with unit diameter. The general solution for the case of zero body forces but with inhomogeneous boundary conditions has been discussed by Palaniappan *et al.* (1992) and Padmavathi *et al.* (1998).

THEOREM 1 (Creeping flow in a sphere). *If $\boldsymbol{f}$ is a smooth vector field in the sphere $\{0\leqslant r\leqslant\frac{1}{2}\}$, then the solution of the Stokes problem*

$$\nabla\cdot\boldsymbol{u} = 0, \tag{3.7a}$$

$$\boldsymbol{f} = -\nabla p + \nabla^2\boldsymbol{u}, \tag{3.7b}$$

with $\boldsymbol{u} = \boldsymbol{0}$ on $r=\frac{1}{2}$ is

$$\boldsymbol{u} = (\nabla\times)^2(\mathscr{P}[\boldsymbol{u}]\boldsymbol{r}) + \nabla\times\mathscr{T}[\boldsymbol{u}]\boldsymbol{r}, \tag{3.8}$$

$$p = -\mathscr{S}[\boldsymbol{f}] - s + \text{a constant}, \tag{3.9}$$

where $\mathscr{P}[\boldsymbol{u}]$, $\mathscr{T}[\boldsymbol{u}]$ and s are scalar fields satisfying

$$\nabla^4\mathscr{P}[\boldsymbol{u}] = \nabla^2\mathscr{P}[\boldsymbol{f}-\boldsymbol{f}^{(S)}] \quad (0\leqslant r<\tfrac{1}{2}), \tag{3.10a}$$

$$\mathscr{P}[\boldsymbol{u}] = \boldsymbol{r}\cdot\nabla\mathscr{P}[\boldsymbol{u}] = 0 \quad (r=\tfrac{1}{2}), \tag{3.10b}$$

$$\nabla^2 \mathscr{T}[\boldsymbol{u}] = \mathscr{T}[\boldsymbol{f} - \boldsymbol{f}^{(S)}] \quad (0 \leqslant r < \tfrac{1}{2}), \tag{3.11a}$$

$$\mathscr{T}[\boldsymbol{u}] = 0 \quad (r = \tfrac{1}{2}), \tag{3.11b}$$

$$\nabla^2 s = 0 \quad (0 \leqslant r < \tfrac{1}{2}), \tag{3.12a}$$

$$\boldsymbol{r} \cdot \nabla s = \boldsymbol{r} \cdot (\nabla\times)^4 (\mathscr{P}[\boldsymbol{u}]\boldsymbol{r}) \quad (r = \tfrac{1}{2}), \tag{3.12b}$$

and $\mathscr{S}[\boldsymbol{f}]$, $\mathscr{P}[\boldsymbol{f} - \boldsymbol{f}^{(S)}]$ *and* $\mathscr{T}[\boldsymbol{f} - \boldsymbol{f}^{(S)}]$ *are scalars from the decomposition of* $\boldsymbol{f}$ *described in Lemma 1.*

Proof. The theorem is proved if it can be shown that the velocity field, $\boldsymbol{u}$, is solenoidal and vanishes on the boundary, and that the field equation is satisfied.

The divergence of $\boldsymbol{u}$ vanishes automatically since $\boldsymbol{u}$ is expressed as the sum of its poloidal and toroidal parts.

Both the poloidal and toroidal parts of $\boldsymbol{u}$ vanish on the surface, by the boundary conditions on $\mathscr{P}[\boldsymbol{u}]$ and $\mathscr{T}[\boldsymbol{u}]$ (§ 3.3). Therefore the boundary condition on $\boldsymbol{u}$ is satisfied.

That the equation of motion is satisfied follows if its residual is solenoidal and irrotational and has zero normal component on the surface $r = \frac{1}{2}$, since these conditions imply that the residual is zero throughout the sphere (Lamb 1932, pp. 37–41). By substitution, and the use of the properties of the decomposition described above and the following identity (Moffatt 1978, p. 19) for any scalar s:

$$(\nabla\times)^3 (\boldsymbol{r}s) = -\nabla \times (\boldsymbol{r}\nabla^2 s), \tag{3.13}$$

the required vanishing of the divergence and curl of the residual may be verified readily; see McBain (1999*b*) for details. □

4. Results

4.1. *Base solution and first-order temperature correction*

Using the method of § 3, the following results may be obtained (in order):

$$T_0 = r \sin\theta \cos\phi, \tag{4.1}$$

$$\boldsymbol{u}_0 = \frac{r}{80} \left(1 - 4r^2\right) \sin\theta \hat{\boldsymbol{\phi}}, \tag{4.2}$$

$$T_1 = \frac{Pr}{44\,800} r(1 - 4r^2)(9 - 20r^2) \cos\eta. \tag{4.3}$$

The first-order approximation to the temperature field, $T_0 + Gr\, T_1$, is contoured for various values of the Rayleigh number, $Ra \equiv Gr\, Pr$, in figure 2. By $Ra = 13\,000$, the approximation has begun to exhibit internal extrema, which is impossible for the full solution (McBain 2001). Figure 2(*a–c*) should not be taken as representing the solution of (2.1) at any particular Grashof number – a full numerical solution would be far more suitable for that, for which see McBain & Stephens (2000). Its use, rather, is to indicate the qualitative effect of the first-order correction, T_1, and the asymptotic behaviour of the temperature field.

Some features of convection in vertical cavities, for example as seen in the interferograms of Eckert & Carlson (1961), are, however, evident in figure 2, even at this low order: the stretching of the level curves at the departure 'corners', meaning the quadrants $xy > 0$; steepening of the horizontal gradients at the starting 'corners', $xy < 0$; and the beginnings of a stable vertical stratification in the core.

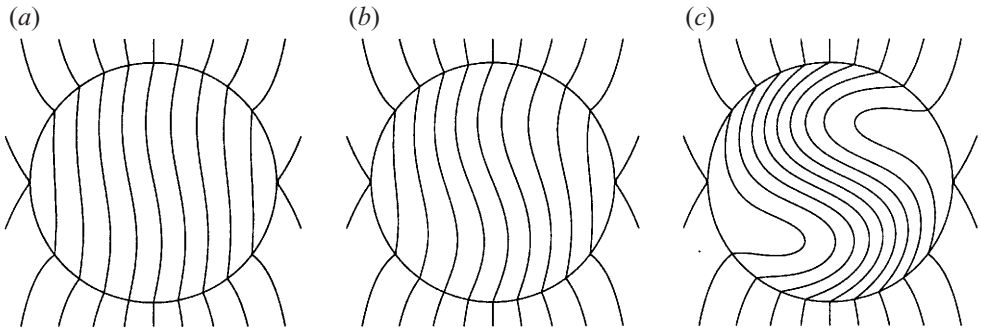

FIGURE 2. Temperature in the plane $z = 0$ to first order, $T_0 + Gr\ T_1$, for Ra of (*a*) 1000, (*b*) 2000, and (*c*) 10 000. Contours at $T = -0.5\,(0.1)\,0.5$.

Visual comparison of figure 2 with figure 4 of McBain & Stephens (2000) reveals that $T_0 + Gr\ T_1$ provides an excellent description of T for $Gr\,Pr$ up to about 2000 for $Pr = 0.7$. For larger Prandtl numbers accuracy at this Rayleigh number would be better still, since the present results are asymptotic in Gr.

4.2. *First-order flow corrections*

It is convenient to decompose the first-order flow into the parts due to inertia and buoyancy: $\boldsymbol{u}_1 = \boldsymbol{u}_{1I} + \boldsymbol{u}_{1B}$, where $\boldsymbol{u}_{1I}$ and $\boldsymbol{u}_{1B}$ are both divergence-free, vanish at the boundary and satisfy

$$\boldsymbol{u}_0 \cdot \nabla \boldsymbol{u}_0 = -\nabla p_{1I} + \nabla^2 \boldsymbol{u}_{1I}, \tag{4.4}$$

$$-T_1 \hat{\boldsymbol{f}} = -\nabla p_{1B} + \nabla^2 \boldsymbol{u}_{1B}. \tag{4.5}$$

The inertia force contains the single term $\boldsymbol{u}_0 \cdot \nabla \boldsymbol{u}_0$. Since only the azimuthal component of $\boldsymbol{u}_0$ is non-zero, and since it is independent of ϕ, it reduces to

$$\boldsymbol{u}_0 \cdot \nabla \boldsymbol{u}_0 = -\frac{(\hat{\boldsymbol{\phi}} \cdot \boldsymbol{u}_0)^2}{r}\,\hat{\boldsymbol{r}} - \frac{(\hat{\boldsymbol{\phi}} \cdot \boldsymbol{u}_0)^2 \cot\theta}{r}\,\hat{\boldsymbol{\theta}}. \tag{4.6}$$

These are precisely the terms of the equation of motion referred to in § 1.1. They are proportional to the square of the component of velocity about the axis and inversely proportional to the distance from the axis: they represent the centrifugal force.

The first-order flow corrections are

$$\boldsymbol{u}_{1I} = \nabla \times \nabla \times \frac{r^2(1-4r^2)^2\,(28r^2-19)}{638\,668\,800}\,(3\cos^2\theta - 1)\boldsymbol{r}, \tag{4.7}$$

$$\boldsymbol{u}_{1B} = Pr\,\nabla \times \nabla \times \frac{r^2(1-4r^2)^2\,(23-20r^2)(3\cos^2\eta - 1)}{638\,668\,800}\,\boldsymbol{r}. \tag{4.8}$$

Both $\boldsymbol{u}_{1I}$ and $\boldsymbol{u}_{1B}$ are poloidal and axisymmetric (relative to the z- and y-axes, respectively); they can both, therefore, be represented by their streamlines in a meridian plane. This is done in figure 3.

The first-order correction to the flow field due to buoyancy is similar to that in a long axially heated horizontal tube (Bejan & Tien 1978). The cause is the same: the redistribution of buoyancy forces by the primary flow leaves the lightest fluid directly under the centre of the cavity's ceiling. This leads to a vertical flow, which parts at the ceiling and moves outward and downward along the confining walls before returning inward along the horizontal mid-plane. The reverse process occurs in the lower hemisphere.

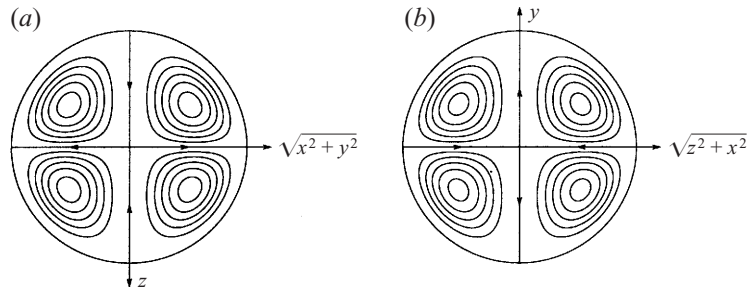

FIGURE 3. Streamlines in meridian planes of the first-order flow corrections due to (*a*) inertia, $\boldsymbol{u}_{1I}$, and (*b*) buoyancy $\boldsymbol{u}_{1B}$.

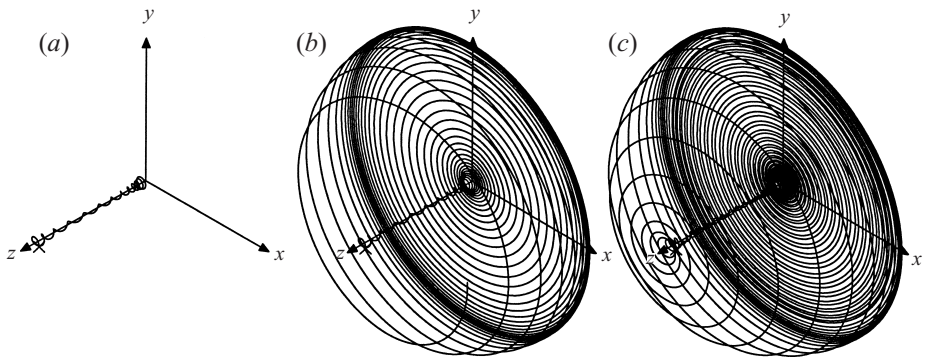

FIGURE 4. The trace of a particle released at the point $r = 0.45$, $\theta = \phi = 0.05$, marked $\times$, into the flow $\boldsymbol{u}_0 + Gr\,\boldsymbol{u}_1$ with $Ra = 1000, Pr = 0.7$ after a dimensionless time interval (units of $D^2/\nu\,Gr$) of (*a*) 10 000, (*b*) 240 000, and (*c*) 360 000.

The result of this section supports the conclusion of Mallinson & de Vahl Davis (1977) that the thermal correction to the flow field ultimately depends on the Grashof and Prandtl numbers in the combination $Gr\,Pr$.

4.2.1. *Particle tracks*

The three-dimensional nature of the flow is illustrated in figure 4 by the locus of a particle released into the first-order approximation to the steady flow at $Ra = 1000$ and $Pr = 0.7$. The release point, $r = 0.45$, $\theta = \phi = 0.05$, is marked with an $\times$. The subfigures are a sequence of snapshots, obtained by numerical integration of the velocity field. The boundary of the sphere is not shown for clarity, but the Cartesian axes are only shown within the domain. Again, the particle tracks should not be taken as indicative of the true solution at $Ra = 1000$ and $Pr = 0.7$, although comparison with the numerical solution of McBain & Stephens (2000) suggests that it is visually indistinguishable. Further, the resemblance of the tracks to those in a cuboid produced from the numerical solutions of the full Boussinesq equations of Mallinson & de Vahl Davis (1973, 1977) is startling. The reader is urged to compare figure 4 with their figures, some of which were reproduced by de Vahl Davis (1998) and Gebhart *et al.* (1988, p. 775).

4.2.2. *On the closure of streamlines*

The reason why the particle does not return to its starting point after a single 'traverse' of the streamsurface is not numerical error. In discussing their computed

streamlines in a cuboid, Mallinson & de Vahl Davis (1977), concluded that the streamlines must be closed, but pointed out that 'multiple traverses on the same surface without streamline intersection are, however, possible and cannot be rejected *a priori*'. In fact, it may be demonstrated that it is entirely (kinematically and topologically) possible for a particle to travel an infinite distance in a steady flow field without returning to its starting point.

Consider the family of circles formed by the intersection of the surface of a torus and the family of cones coaxial with the torus and with vertex at the torus's centre. This family of curves satisfies the kinematic and topological requirements of a set of streamlines free from critical points; it is, for example, homeomorphic to the family of streamlines on a typical streamtube of the creeping flow, $\boldsymbol{u}_0$. Now cut the surface of the torus with a semi-plane bounded by its axis, twist one of the ends so-formed and then rejoin the surface and streamlines. Unless a rational number of twists were applied to the end, the particle would never return to its starting point, even though it remains on the same finite surface (cf. the discussion of force-free magnetic field lines by Moffatt 1978, p. 30).

The addition of the correction for inertia to the creeping flow has a similar effect to the above cutting, twisting and rejoining operation.

5. Conclusions

The flow to first order in the Grashof number in a spherical cavity subjected to a horizontal temperature gradient is seen to embody the two mechanisms adduced by Mallinson & de Vahl Davis (1973, 1977) for spanwise flow in a horizontally heated cuboid: the thermal effect and the inertial effect. The terms in the governing equations responsible for these mechanisms are evident in the analytical derivation and expression of these corrections for the sphere. Although equivalent solutions for the cuboid have not yet been obtained, the same terms would be active.

The analysis has also clarified the conditions under which the corrections would not occur. The buoyancy effect vanishes with the Rayleigh number and also vanishes if the flow is vertical, as in the tall cavity solutions of McBain (1999*a*) since there is then no disturbance of the temperature fields. The inertia effect vanishes if the streamlines are parallel, since the force is inversely proportional to their radius of curvature. It also vanishes with the Grashof number; in dimensional terms the force is proportional to the square of the primary velocity.

The conclusion that 'for rolls adjacent to a solid boundary ... as $Ra \to 0$, the axial flow asymptotes to a constant fraction of the cross-sectional flow, a fraction which is certainly not negligible, especially for $Pr \sim 1$' (de Vahl Davis 1998; paraphrasing Mallinson & de Vahl Davis 1977) must be regarded as incorrect.

The preceding analysis in no way precludes non-zero spanwise components of velocity at $Gr = 0$ in a cuboid, since there may be other mechanisms involved. The creeping flow in a cuboid, for example, must, unlike that in a sphere, have a poloidal part. The streamlines of a toroidal flow are confined to concentric spheres but infinitesimally close to a non-critical point of a solid wall, a solenoidal flow must be parallel to the wall.

It is a pleasure for the author to acknowledge the helpful conversations with Don Close, Harry Suehrcke, Jonathan Harris, Eric Peterson and Lance Bode. Further thanks are due to Dr Harris for suggesting the problem.

REFERENCES

Backus, G. 1986 Poloidal and toroidal fields in geomagnetic field modeling. *Rev. Geophys.* **24**, 75–109.

Bejan, A. & Tien, C. L. 1978 Fully developed natural counterflow in a long horizontal pipe with different end temperatures. *Intl J. Heat Mass Transfer* **21**, 701–708.

Chadwick, P. & Trowbridge, E. A. 1967 Elastic wave fields generated by scalar wave functions. *Proc. Camb. Phil. Soc. Math. Phys. Sci.* **63**, 1177–1187.

Eckert, E. R. G. & Carlson, W. O. 1961 Natural convection in an air layer enclosed between two vertical plates with different temperatures. *Intl J. Heat Mass Transfer* **2**, 106–120.

Elsasser, W. M. 1946 Induction effects in terrestrial magnetism. I. Theory. *Phys. Rev.* **69**, 106–116.

Gebhart, B., Jaluria, Y., Mahajan, R. L. & Sammakia, B. 1988 *Buoyancy-Induced Flows and Transport*, textbook edn. Hemisphere.

Hiller, W. J., Koch, S. & Kowalewski, T. A. 1989 Three-dimensional flow structures in laminar natural convection in a cubic enclosure. *Expl Thermal Fluid Sci.* **2**, 34–44.

Lamb, H. 1932 *Hydrodynamics*, 6th edn. Cambridge University Press.

Lewis, J. A. 1950 Free convection in commerical insulating materials. PhD thesis, Brown University, Providence.

Mallinson, G. D. & de Vahl Davis, G. 1973 The method of the false transient for the solution of coupled elliptic equations. *J. Comput. Phys.* **12**, 435–461.

Mallinson, G. D. & de Vahl Davis, G. 1977 Three-dimensional natural convection in a box: A numerical study. *J. Fluid Mech.* **83**, 1–31.

McBain, G. D. 1999*a* Fully developed laminar buoyant flow in vertical cavities and ducts of bounded section. *J. Fluid Mech.* **401**, 365–377.

McBain, G. D. 1999*b* Vapour transport across gas-filled enclosures. PhD thesis, James Cook University, Townsville.

McBain, G. D. 2001 Spatial extrema of advected scalars. *Intl J. Heat Mass Transfer* **44**, 863–865.

McBain, G. D. & Stephens, D. W. 2000 Low Grashof number convective heat transfer across a spherical cavity. In *Heat and Mass Transfer Australasia 2000* (ed. G. B. Brassington & J. C. Patterson), pp. 231–237. Chalkface.

Moffatt, H. K. 1978 *Magnetic Field Generation in Electrically Conducting Fluids.* Cambridge University Press.

Morrison, G. L. & Tran, V. Q. 1978 Laminar flow structure in vertical free convective cavities. *Intl J. Heat Mass Transfer* **21**, 203–213.

Ostrach, S. 1988 Natural convection in enclosures. *J. Heat Transfer* **110**, 1175–1190.

Ostroumov, G. A. 1958 Free convection under the conditions of the internal problem. *Tech. Rep.* TM 1407. NACA (transl. S. Reiss).

Padmavathi, B. S., Raja Sekhar, G. P. & Amaranth, T. 1998 A note on complete general solutions of Stokes equations. *Q. J. Mech. Appl. Maths* **51**, 383–388.

Palaniappan, D., Nigam, S. D., Amaranth, T. & Usha, R. 1992 Lamb's solution of Stokes's equations: A sphere theorem. *Q. J. Mech. Appl. Maths* **45**, 47–56.

Pao, H.-P. 1970 A numerical computation of a confined rotating flow. *Trans. ASME: J. Appl. Mech.* **37**, 480–487.

Rayleigh, Lord 1913 On the motion of a viscous fluid. *Phil. Mag.* **26**, 776–786.

de Vahl Davis, G. 1998 Unnatural natural convection. In *Heat and Mass Transfer Australasia 1996* (ed. E. Leonardi & C. V. Madhusudana), pp. 1–16. Begell House.